1.0, with the best value being less than 0.1. If carriers were being trapped out at the grain boundaries, shorter decay times at higher fields would be expected, but this was not observed. Rather, the decay times were independent of the field in all samples.

Although both types of films appear to contain a high density of traps, their nature and energy distribution appear to be different, on the basis of the shape of the decays. The slow tail in the dc films is likely due to carrier detrapping, which involves the capture of electrons (or holes) by a shallow trap level. Thermal excitation then brings these carriers back into the conduction (or valence) band. In the samples with little or no tail, the trap levels may be deep enough that detrapping becomes insignificant. It is possible that just small changes in growth parameters between films is enough to alter the depths and distributions of the traps. It is common in polycrystalline materials to find large densities of traps, either discrete or continuous in energy distribution. An exponential distribution of traps in microwave diamond films has been observed (*12*), and others have reported high densities of acceptor states distributed over several electron volts above the valence band (*28, 29*). In natural single-crystal diamonds, nitrogen impurities play an important role in carrier recombination (*24*). In the case of the polycrystalline diamond films, high densities of defects, most notably dislocations, stacking faults, twins (*30, 31*), and impurities, have been observed, which can act as trapping and recombination sites. In future investigations it will be necessary to relate these structural defects and their densities with measured electrical properties.

Although the electrical properties of polycrystalline diamond are steadily improving, the material is still much poorer in quality than single-crystal natural diamonds. For example, the low-density mobility of the best films studied here is between 10 to 100 times less than that of single-crystal natural diamond. In order to use CVD diamond for device applications, the defect densities must be lowered to improve both lifetime and mobility. The material is promising, however, because of the ability to control the processing. Recent improvements in the quality of the films are encouraging. Epitaxial diamond films have been deposited with properties very close to those of the diamond substrate (*32*), demonstrating that the CVD technique is capable of producing high-quality diamond.

REFERENCES AND NOTES

1. R. Berman, in *Properties of Diamond*, J. E. Field, Ed. (Academic Press, San Diego, CA, 1979), pp. 3–22.
2. J. E. Field, Ed., *ibid.*
3. C. Canali *et al.*, *Nucl. Instrum. Methods* **160**, 73 (1979).
4. G. A. Baraff, *Phys. Rev. A* **133**, 26 (1964).
5. J. Fontanella, R. L. Johnston, J. H. Colwell, C. Andeen, *Appl. Opt.* **16**, 2949 (1977).
6. W. B. Wilson, *Phys. Rev.* **127**, 1549 (1962).
7. R. W. Keyes, *Proc. IEEE* **60**, 225 (1972).
8. A. Johnson, *RCA Rev.* **26**, 163 (1965).
9. G. S. Gildenblat, S. A. Grot, A. Badzian, *Proc. IEEE* **79**, 647 (1991).
10. W. A. Yarbrough and R. Messier, *Science* **247**, 688 (1990); W. Zhu, B. R. Stoner, B. E. Williams, J. T. Glass, *Proc. IEEE* **79**, 621 (1991).
11. M. I. Landstrass and K. V. Ravi, *Appl. Phys. Lett.* **55**, 975 (1989).
12. S. Ashok, K. Srikanth, A. Badzian, T. Badzian, R. Messier, *ibid.* **50**, 763 (1987).
13. Doping, particularly *p*-type, has been achieved with some success, but dopants tend to form deep levels, requiring high concentrations of dopants that can severely limit the carrier mobility.
14. D. R. Kania *et al.*, *J. Appl. Phys.* **68**, 124 (1990).
15. L. S. Pan, P. Pianetta, D. R. Kania, O. L. Landen, K. V. Ravi, in *OSA Proceedings on Picosecond Electronics and Optoelectronics*, T. C. L. G. Sollner and D. M. Bloom, Eds. (Optical Society of America, Washington, DC, 1989), pp. 170–174; L. S. Pan *et al.*, *Electrochem. Soc. Proc.* **89-12**, 424 (1989).
16. E. L. Palik, Ed., *Handbook of Optical Constants of Solids* (Academic Press, Orlando, FL, 1985), pp. 665–673.
17. D. S. Knight and W. B. White, *J. Mater. Res.* **4**, 385 (1989).
18. J. W. Ager III, D. K. Veirs, G. M. Rosenblatt, *Phys. Rev. B* **43**, 6491 (1991).
19. O. L. Landen, M. D. Perry, E. M. Campbell, *Phys. Rev. Lett.* **60**, 1270 (1988).
20. P. S. Panchhi and H. M. van Driel, *IEEE J. Quantum Electron.* **QE-22**, 101 (1986).
21. L. S. Pan, D. R. Kania, P. Pianetta, S. Han, O. L. Landen, in preparation.
22. A. G. Redfield, *Phys. Rev.* **94**, 526 (1954).
23. E. A. Konorova and S. A. Shevchencko, *Sov. Phys. Semicond.* **1**, 299 (1967).
24. L. S. Pan, D. R. Kania, P. Pianetta, O. L. Landen, *Appl. Phys. Lett.* **57**, 623 (1990).
25. K. Okano, personal communication.
26. K. Okano *et al.*, in *New Diamond Science and Technology*, R. Messier, J. T. Glass, J. E. Butler, R. Roy, Eds. (Materials Research Society, Pittsburgh, 1990), pp. 917–924.
27. K. Nishimura, personal communication.
28. K. Okumura, J. Mort, M. Machonkin, *Appl. Phys. Lett.* **57**, 1907 (1990).
29. J. Mort, M. A. Machonkin, K. Okumura, *ibid.* **59**, 455 (1991).
30. B. E. Williams and J. T. Glass, *J. Mater. Res.* **4**, 373 (1989).
31. J. L. Kaae, P. K. Gantzel, J. Chin, W. P. West, *ibid.* **5**, 1480 (1990).
32. L. S. Pan *et al.*, in preparation.

33. This work was performed under the auspices of the U.S. Department of Energy by Lawrence Livermore National Laboratories under contract W-7405-ENG-48 and was also supported by the Stanford Synchrotron Radiation Laboratory, which is supported by the U.S. Department of Energy, Office of Basic Energy Science, Division of Chemical Sciences. In this research P.P. was supported by that office's Division of Material Science. M.L. was supported by the U.S. Air Force at Eglin Air Force Base. The work at Lawrence Berkeley Laboratories was supported by the Director, Office of Energy Research, U.S. Department of Energy, under contract DE-AC-03-76SF00098.

30 September 1991; accepted 6 December 1991

Compressibility of M_3C_{60} Fullerene Superconductors: Relation Between T_c and Lattice Parameter

OTTO ZHOU, GAVIN B. M. VAUGHAN, QING ZHU,
JOHN E. FISCHER,* PAUL A. HEINEY, NICOLE COUSTEL,
JOHN P. MCCAULEY, JR., AMOS B. SMITH III

X-ray diffraction and diamond anvil techniques were used to measure the isothermal compressibility of K_3C_{60} and Rb_3C_{60}, the superconducting, binary alkali-metal intercalation compounds of solid buckminsterfullerene. These results, combined with the pressure dependence of the superconducting onset temperature T_c measured by other groups, establish a universal first-order relation between T_c and the lattice parameter a over a broad range, between 13.9 and 14.5 angstroms. A small second-order intercalate-specific effect was observed that appears to rule out the participation of intercalate-fullerene optic modes in the pairing interaction.

A NUMBER OF ISOSTRUCTURAL BInary and pseudobinary alkali metal–C_{60} superconductors have been discovered that have onset temperatures T_c ranging from 18 to 33 K (*1*). Their general formulas are $M_{3-x}M'_xC_{60}$, and their face-centered-cubic lattice parameters a range from 14.25 to 14.49 Å at atmospheric pressure and 300 K. A monotonic increase of T_c with alkali size is inferred from an empirical linear correlation between T_c and a at constant pressure (*1*). Moreover, T_c decreases with increasing pressure for the binary compounds with M = K (*2, 3*) and Rb (*4*), and the two sets of $T_c(P)$ data can be superposed by a relative shift of the pressure scales (*4*). These results both suggest that T_c depends only on the overlap between near-neighbor C_{60} molecules and not explicitly on the

---

O. Zhou, Q. Zhu, J. E. Fischer, N. Coustel, Laboratory for Research on the Structure of Matter and Department of Materials Science and Engineering, University of Pennsylvania, Philadelphia, PA 19104.
G. B. M. Vaughan and P. A. Heiney, Laboratory for Research on the Structure of Matter and Department of Physics, University of Pennsylvania, Philadelphia, PA 19104.
J. P. McCauley, Jr., and A. B. Smith III, Laboratory for Research on the Structure of Matter and Department of Chemistry, University of Pennsylvania, Philadelphia, PA 19104.

---

*To whom correspondence should be addressed.

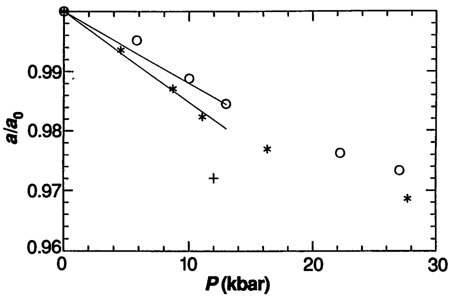

Fig. 1. Fractional reduction of lattice parameter a/a_0 versus pressure P: (○), K_3C_{60}; (*), Rb_3C_{60}; and (+), pure C_{60} (*10*). The experimental errors in a and P are ±0.002 Å and ±0.3 kbar, respectively. Solid lines are linear fits to the data points up to 13 kbar.

nature of the intercalate (*1, 4*). In the context of weak-coupling Bardeen-Cooper-Schrieffer (BCS) superconductivity, both results are interpreted to mean that $N(E_F)$, the density of states at the Fermi energy, increases with increasing intermolecular separation because of reduced orbital overlap and conduction electron bandwidth (assuming that the number of electrons transferred to the conduction band or bands per intercalate is the same for all alkali metals and is independent of P). In the weak-coupling BCS model, $kT_c = \hbar\omega_{ph}e^{-1/VN(E_F)}$, where k is the Boltzmann constant, $\hbar\omega_{ph}$ is a phonon energy, and V is the electron-phonon coupling constant. The dependence of T_c on a is implicit in $N(E_F)$, so the universality of $T_c(a)$ implies that ω_{ph} and V are independent of P, that is, the total differential dT_c/dP is dominated by a single term $[\partial T_c/\partial a][da/dP]$. With the additional assumption of no pressure-induced structural transitions, Fleming *et al.* (*1*) predicted a universal compressibility value for all of the isostructural compounds. Similarly, Sparn *et al.* (*4*) predicted a compressibility value for Rb_3C_{60} by scaling T_c and a for the two binary compounds.

We measured the pressure dependence of a for K_3C_{60} and Rb_3C_{60} at 300 K using x-ray diffraction. This experiment permits a direct test of the validity of the assumptions noted above. Scaling our $a(P)$ data point-by-point with the measured $T_c(P)$ up to 28 kbar permits us to extend the T_c versus a correlation down to T_c and a values as low as 6 K and 13.9 Å, respectively. The overall behavior is still generally consistent with a universal phenomenon that depends only on intermolecular separation. Not surprisingly, the correlation is no longer linear over the larger range of parameters. Our analysis also reveals a small, second-order, metal-specific effect, the sense of which allows us to rule out pairing mediated by phonons involving the alkali ions. This secondary effect in the $T_c(a)$ correlation is revealed by the observation that the compressibilities of K_3C_{60} and Rb_3C_{60} are significantly different.

Powder samples of M_3C_{60} were prepared by the dilution technique described in detail elsewhere (*5*). Equimolar amounts of >99.5% pure C_{60} and saturation-doped M_6C_{60} (*6*) powders were mixed together in a dry box by grinding and then sealed in evacuated pyrex tubes. These were first heated to 250°C for 24 hours and then annealed in two steps, first at 350°C for 24 hours and then at 400°C for 1 hour. We have previously established by x-ray diffraction that this procedure reproducibly gives single-phase material (*5, 7*). Diamagnetic shielding measurements of uncompacted powders gave T_c values and shielding fractions of 29.6 K and 56% for Rb_3C_{60} and 19.3 K and 38% for K_3C_{60}, respectively (*5*).

X-ray diffraction experiments were carried out with synchrotron radiation at the National Synchrotron Light Source X10B beamline. The vertical diffractometer was equipped with a bent Si(111) monochromator crystal for horizontal focusing and a platinum-coated zerodur mirror for vertical focusing and was set for a wavelength λ of 0.947 Å. The resolution ΔQ was of order 0.0035 $Å^{-1}$ full-width at half-maximum ($Q = 4\pi\sin\theta/\lambda$). Pressures up to 28 kbar were provided by a Merrill-Bassett diamond anvil cell by using mineral oil or pentane-isopentane as hydrostatic media (*8*). We added CaF_2 powder to the cell and measured pressure from its lattice parameter (determined from three reflections) and the empirical equation of state (*9*). Four strong Bragg reflections of M_3C_{60} (111, 311, 222, and 420) were recorded at each pressure. No other Bragg reflections were observed in this range of scattering angles up to the maximum pressure. The four measured peaks were fitted with a single lattice parameter, and mixed Gaussian-Lorentzian intensity functions to obtain a at each pressure. A 2θ zero-offset correction was measured at each pressure by recording a CaF_2 reflection with negative scattering angle.

The fractional reduction in lattice parameter a/a_0 with increasing pressure for the two M_3C_{60} compounds is shown in Fig. 1, as well as an earlier result for pure C_{60} (*10*). The contraction is linear up to ~13 kbar within experimental error, from which we derive average linear compressibilities $d\ln a/dP$ of $1.20 \pm 0.09 \times 10^{-3}$ and $1.52 \pm 0.09 \times 10^{-3}$ $kbar^{-1}$ for K_3C_{60} and Rb_3C_{60}, respectively. These are both less than the value $2.3 \pm 0.2 \times 10^{-3}$ $kbar^{-1}$ for pure C_{60} based on the single data point. The stiffening effect of alkali intercalation is attributed to an increase in lattice energy resulting from the ionic guest-host interaction (*1, 2*). A similar effect occurs in intercalated graphite (*11*). K_3C_{60} and Rb_3C_{60} both become stiffer above 13 kbar, as shown by the flattening out of a/a_0 versus P at higher pressures. This stiffening also occurs in pure C_{60} (*12*).

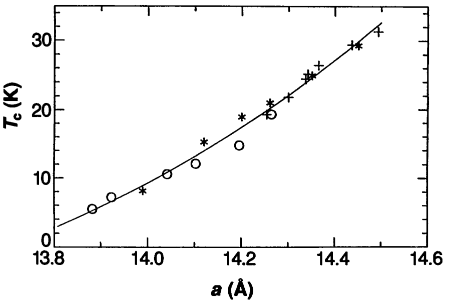

Fig. 2. Superconducting transition temperature versus lattice parameter. The $a(P)$ data from Fig. 1 was converted to $T_c(a)$ by using the raw $T_c(P)$ data of (*2*) and (*4*): (○), K_3C_{60}; (*), Rb_3C_{60}; and (+), directly measured points from a number of $M_{3-x}M'_xC_{60}$ compounds at 300 K and 1 bar (*1*). Solid curve is a quadratic fit.

Our measured compressibility for Rb_3C_{60} agrees fairly well with the predicted value 1.7×10^{-3} $kbar^{-1}$ (*4*). Similarly, the average of our volume compressibilities for K_3C_{60} and Rb_3C_{60}, $4.08 \pm 0.27 \times 10^{-3}$ $kbar^{-1}$, is consistent with values predicted from the empirical linear relation between T_c and a (*1*) and the two measurements of dT_c/dP (*2, 3*), namely 4.7×10^{-3} and 4.0×10^{-3} $kbar^{-1}$, respectively. These comparisons show that, for a given compound, dT_c/dP is indeed dominated by the term $[\partial T_c/\partial a][da/dP]$. Therefore, within weak-coupling BCS theory and linear approximations for $T_c(P)$ and $a(P)$, any pressure dependences of phonon energies or the coupling constant have negligible effects on T_c below 13 kbar.

The results of converting all of the $a(P)$ data in Fig. 1 point-by-point to $T_c(a)$ are shown in Fig. 2. We interpolated between the $T_c(P)$ data points of Sparn *et al.* (*2, 4*) to obtain T_c's at the corresponding P's. This procedure goes beyond the approximation of linear $T_c(P)$ and $a(P)$ at low P but is not rigorously correct because the T_c values were measured near 0 K whereas the P-dependent a values were measured at 300 K. Also plotted in Fig. 2 are Fleming's $T_c(a)$ data at 1 bar for seven different compounds. The $T_c(P)$ and $a(P)$ measurements were performed in two different laboratories, which does not compromise the relative accuracy of the $T_c(a)$ correlations for K- and Rb-doped compounds because both $T_c(P)$ measurements were performed in the same laboratory, as were both $a(P)$ measurements. On the other hand, the absolute relation of the two pressure-dependent data sets to Fleming's 1-bar data is subject to systematic uncertainties. There is good agreement between the two data points for K_3C_{60} (19 K and 14.24 Å) and Rb_3C_{60} (29.6 K and 14.42 Å) at 1 bar. The absolute uncertainties (±0.5 K %) are smaller than the plot symbols.

The solid curve in Fig. 2 indicates that all three data sets are represented reasonably well by a single quadratic function. We conclude that the proposed universal correlation between T_c and a is correct to first order. The positive sign of the quadratic term may serve as a detailed test of competing models, for example, from the dependence on a of the parameters in the MacMillan formula.

Our data also reveal a small second-order intercalate-specific contribution to $T_c(a)$. From Fig. 1, the compressibilities of K_3C_{60} and Rb_3C_{60} are not identical, as would be required by a strictly universal correlation. The three data sets in Fig. 2 can also be reasonably well described by individual linear segments. The "universal" slope of Fleming's directly measured values is 50 K $Å^{-1}$, which is quite close to our value of 45 ± 1 K $Å^{-1}$ for Rb_3C_{60} but significantly larger than our value of 33 ± 2 K $Å^{-1}$ for K_3C_{60}. The intercalate-specific effect is only significant at small a, that is, at large intermolecular overlap.

The sense of this effect is inconsistent with a proposal that metal-C_{60} optic modes are responsible for the pairing interaction (*13*). In this hypothesis, superconductivity arises from strong coupling to relatively low-frequency modes rather than from weak coupling to the intramolecular vibrations, which lie at higher frequencies (*14, 15*). If we assume a linear contribution to $T_c(a)$ from the $e^{1/VN(E_F)}$ factor independent of chemical composition, and that the important coupling phonons are zone-boundary optic modes involving planes of M_3 and of C_{60} (*13*), there would be an additional scaling of T_c as $\sqrt{(1/m)}$, where m is the reduced mass. This scaling would be in the ratio 14:10 for K_3C_{60} and Rb_3C_{60}, the inverse of the observed 33:45 ratio of slopes.

There are several possible origins for the small intercalate-specific contribution. The first is suggested by the complex Fermi surface of K_3C_{60} (*16*). In addition to bandwidth variations, which depend directly on the lattice parameter, the volume of the Fermi surface may be subtly different for different intercalates, or may vary with lattice parameter or pressure, or both effects could occur. Another possibility is a pressure-induced phase transition involving molecular orientations. In pure C_{60}, free molecular rotations freeze out at $T_{mo} = 249$ K at 1 bar, locking into specific orientations with respect to the crystal axes (*17*), and T_{mo} decreases rapidly with increasing P (*18, 19*). An x-ray study of K_3C_{60} indicates two equally populated molecular orientations at 300 K and 1 bar (*20*), and a nuclear magnetic resonance study of Rb_3C_{60} gives evidence for a transition near 300 K (*21*). It is therefore likely that M_3C_{60} transforms to an orientationally ordered phase at 300 K within the P range of the present data, which could affect our analysis by introducing discontinuities in $a(P)$ or by slightly modifying the Fermi surface. The diffraction signature of this transition is quite subtle in C_{60} (*17*) and would have been undetectable in the present experiments. More data at the extremes of a would help clarify the situation, for example dT_c/dP and compressibility measurements on Rb_2CsC_{60} (*1*) and extension of the $T_c(P)$ experiments to higher pressure.

REFERENCES AND NOTES

1. R. M. Fleming *et al.*, *Nature* **352**, 787 (1991).
2. G. Sparn *et al.*, *Science* **252**, 1829 (1991).
3. J. E. Schirber *et al.*, *Physica C* **178**, 137 (1991).
4. G. Sparn *et al.*, unpublished results.
5. J. P. McCauley, Jr., *et al.*, *J. Am. Chem. Soc.* **113**, 8537 (1991).
6. O. Zhou *et al.*, *Nature* **351**, 632 (1991).
7. Q. Zhu *et al.*, *Science* **254**, 545 (1991).
8. We first checked that no degradation in x-ray profiles occurred after immersing M_3C_{60} powder in these liquids for several days. Mineral oil was used only below 8 kbar because of its low glass-transition pressure. The disadvantage of pentane-isopentane is its high vapor pressure, which makes it more difficult to seal the cell without trapping voids in the gasket hole.
9. J. Jayaraman, *Rev. Mod. Phys.* **55**, 1 (1983); L. Finger and H. Hazen, *Comparative Chemistry* (Wiley, New York, 1982).
10. J. E. Fischer *et al.*, *Science* **252**, 1288 (1991).
11. H. Zabel, in *Graphite Intercalation Compounds, Topics of Current Physics*, H. Zabel and S. A. Solin, Eds. (Springer-Verlag, Berlin, 1990), pp. 101–156.
12. S. J. Duclos *et al.*, *Nature* **351**, 380 (1991).
13. F. C. Zhang, M. Ogata, T. M. Rice, *Phys. Rev. Lett.* **67**, 3452 (1991).
14. M. Schluter, M. Lannoo, M. Needels, G. Baraff, D. Tomanek, unpublished results.
15. C. M. Varma, J. Zaanen, K. Raghavachari, *Science* **254**, 989 (1991).
16. S. C. Erwin and W. E. Pickett, *ibid.*, p. 842.
17. P. A. Heiney *et al.*, *Phys. Rev. Lett.* **66**, 2911 (1991).
18. G. A. Samara *et al.*, *ibid.* **67**, 3136 (1991).
19. G. Kriza *et al.*, *J. Phys. I (France)* **1**, 1361 (1991).
20. P. W. Stephens *et al.*, *Nature* **351**, 632 (1991).
21. R. Tycko *et al.*, *Science* **253**, 884 (1991).
22. We thank G. Sparn for providing his raw $T_c(P)$ data, M. Y. Jiang for technical assistance, and also K. S. Liang for the use of the X10B beamline. We acknowledge helpful discussion with S. C. Erwin, A. B. Harris, and E. J. Mele. Supported by NSF grants no. DMR-88-19885 and no. DMR-89-01219 and by the Department of Energy, grant no. DE-FC02-86ER45254.

18 November 1991; accepted 2 January 1992

Molecular Dynamics Simulations of Dimer Opening on a Diamond {001}(2×1) Surface

BARBARA J. GARRISON,* ERIC J. DAWNKASKI, DEEPAK SRIVASTAVA,
DONALD W. BRENNER*

Computer simulations of hydrocarbon and related molecules using empirical force fields have become important tools for studying a number of biological and related processes at the atomic scale. Traditional force fields, however, cannot be used to simulate dynamic chemical reactivity that involves changes in atomic hybridization. Application of a many-body potential function allows such reactivity to occur in a computer simulation. Simulations of the reaction of small hydrocarbon molecules adsorbed on a reconstructed diamond {001}(2×1) surface suggest that these hydrocarbons are highly reactive species and that initial stages of diamond growth proceed through a dimer-opening mechanism. Rates estimated from transition state theory of two interconversions between states where the dimer is open and closed are given.

CHEMICAL REACTIONS ARE DEFINED by a changing atomic coordination associated with the breaking and making of bonds. Creation of a microscopic description of the events associated with these processes for small systems (*1*) has been a tour de force for modern chemistry. We understand in exquisite detail reaction mechanisms, quantum mechanical resonances, and final vibrational state distribution of reactions such as F + H_2 → FH + H and H + H_2 → H_2 + H. Analogous accomplishments for large ensembles of atoms and molecules have been slow, however, as the focus of research changes from small molecular systems to large ones. Thus, it is timely to question how reactions proceed in condensed phases. To approach this problem, we have used molecular dynamics (MD) calculations to investigate the diamond film formation from hydrocarbon species.

B. J. Garrison, E. J. Dawnkaski, D. Srivastava, 152 Davey Laboratory, Department of Chemistry, Pennsylvania State University, University Park, PA 16802.
D. W. Brenner, Code 6179, Naval Research Laboratory, Washington, DC 20375.

---

*To whom correspondence should be addressed.